За допомогою числової моделі, розробленої на основі запропонованих фізичної та математичної моделей, виконано моделювання теплоелектричного стану печі Кастнера у процесі графітування електродних заготовок. Верифікація числової моделі показала, що відмінність у температурних полях між даними числового аналізу та фізичного експерименту з урахуванням впливу газифікації не перевищує 4 % в інтервалі температур до 1600 °C

Ключові слова: графітування, електродні заготовки, газифікація, теплоелектричний стан, піч прямого нагріву

С помощью численной модели, разработанной на основе предложенных физической и математической моделей, выполнено моделирование теплоэлектрического состояния печи Кастнера в процессе графитирования электродных заготовок. Верификация численной модели показала, что отличие в температурных полях между данными численного анализа и физического эксперимента с учётом влияния газификации не превышает 4 % в интервале температур до 1600 °C

Ключевые слова: графитирование, электродные заготовки, газификация, теплоэлектрическое состояние, печь прямого нагрева

UDC 621.365.3
DOI: 10.15587/1729-4061.2016.83191

NUMERICAL ANALYSIS OF THE PHYSICAL FIELDS IN THE PROCESS OF ELECTRODE BLANKS GRAPHITIZATION IN THE CASTNER FURNACE

A. Karvatskii
Doctor of Technical Sciences, Professor*
E-mail: anton@rst.kpi.ua
S. Leleka
PhD, Researcher**
E-mail: sleleka@rst.kpi.ua
A. Pedchenko
Postgraduate student*
E-mail: anatolek@rst.kpi.ua
T. Lazariev
PhD, Researcher**
E-mail: t_lazarev@rst.kpi.ua
*Department of Chemical, Polymer and Silicate Engineering***
Research center "Resource-saving technologies"*
***National Technical University of Ukraine "Igor Sikorsky Kyiv Polytechnic Institute"
Peremogy ave., 37, Kyiv, Ukraine, 03056

1. Introduction

Electrode blanks under production-line conditions are graphitized mainly in electric furnaces of resistance by the Castner method (direct heating) or the Acheson method (indirect heating). Large-diameter electrodes (of 600 mm or more) are graphitized in direct heating furnaces that operate by the Castner method.

A characteristic feature of this method is the direct electrothermal heating of electrode blanks with the direct current (DC) and the relatively short duration of the process – about 10–25 hrs [1–3].

The conversion of a carbonaceous material into a graphite structure in the process of graphitization depends on a number of factors, including the material properties of the electrode blanks, the prehistory of heat treatment, the duration of the graphitization process, and the level of the reached temperatures. However, numerous studies show that the main factor that determines the degree of graphitizing the carbonaceous material of electrode blanks is the top temperature: to obtain artificial graphite of sufficient quality, the temperature should be at least 2,200–2,800 °C [3]. Experimental research on such high-temperature processes in a highly aggressive environment of the furnace is extremely complex and labour-intensive [3]. Therefore, to determine the thermoelectric state of the workspace in graphitization furnaces, it has become common to apply methods that are based on the rational use of numerical modelling in conjunction with selective (separate) physical experiments [4, 5].

2. Literature review and problem statement

Our analysis of the studies on the issue of graphitization of electrode products has showed that most of them are dedicated to modelling physical fields in furnaces for indirect heating by the Acheson method.

In [6, 7], it is suggested to use three-dimensional mathematical models of an AC graphitization furnace based on a system of Maxwell equations for complex amplitudes of the magnetic vector and electric potentials, a system of convective heat transfer equations in the Boussinesq approximation, and a thermal conductivity equation. The thermoelectric power state of the graphitization furnace is calculated by using COMSOL MultyPhysics and ANSYS as the software. The calculations are performed by applying the finite element method. The developed model takes into account the temperature dependence of the electromagnetic properties of the conductive elements of the furnace, the effects of displacement, and the external surface effect.

In [8], a method of a numerical evaluation of the electrical parameters of bussed links of current leads of the graphitization furnace with side bus packets is based on the solution of the dual problem for electric and electromagnetic fields. The numerical solution of the problem is achieved by the finite element method with condensation of the finite element mesh in areas with an increased intensity of the magnetic field.

In [9], the effect of the mechanical strength of graphite electrodes is researched under the influence of heat and mechanical stress. The numerical model is based on a two-dimensional axisymmetric problem, using the dependence of the physical properties of the material on temperature. The calculations are performed through the software ABAQUS, using the finite element method.

In [10], it is suggested to use a numerical model of a direct heating furnace for a joint production of graphite products and silicon carbide (SiC). The model also accounts for the dependence of physical properties on the temperature of the material. For the time-dependent thermal calculations, open and free FEPG software is used on the basis of the finite element method.

For the purpose of heat recovery and reduction of the graphitization furnace cool-down period, a solution is suggested in [11] to use tubular heat exchangers in the heat-insulating layer. A corresponding numerical model is offered to describe the task of a joint heat exchange in the furnace and in the heat exchanger and to assess the thermal efficiency of the technical solution.

In [12], there is a description of a technique of a mathematical modelling of physical and chemical processes in manufacturing electrode products in Acheson graphitization furnaces. The study explores the effect of physical and chemical properties of the carbon furnace insulation on the thermal field of the furnace as well as the related field of mass transfer processes and the evolution of gas.

The disadvantages of the above-described numerical models include the lack of consideration of the thermal effects of chemical reactions, vaporization processes, mass transfer and condensation of moisture in bulk materials in the furnace. Also, the physical properties of the bulk material do not depend on the pressure, the geometry of the furnace is simplified, and the numerical models of the physical fields of the furnace are often limited to the area in which there is an assessment of their adequacy.

Thus, the reviewed studies do not take into account the sufficiently important factors that uniquely affect and determine the dynamics of the thermoelectric state of the direct heating furnace during the graphitization of electrode products. Therefore, a promising direction is to develop a mathematical model of the thermoelectric effect of the Castner furnace, which does not contain the enumerated deficiencies.

3. The purpose and objectives of the study

The aim is to undertake a numerical study of the thermoelectric fields of the Castner furnace and to check the adequacy of the physical data of an experiment.

To achieve this goal, it is necessary to do the following tasks:

– to formulate a physical model based on the analysis of the physicochemical processes occurring during the graphitization of electrode products in Castner furnaces;

– to develop mathematical and numerical models of the thermoelectric state of the Castner furnace on the basis of information about the physical properties of the process and the thermal effects of the chemical reactions of gasification, evaporation, condensation, graphite sublimation, and thermoelectric contact interaction between the elements of the furnace design;

– to verify the developed numerical model of the process of graphitizing carbon blanks in the Castner furnace according to the physical experiment.

4. The physical model of the graphitization process

The workspace of the Castner furnace (Fig. 1) is an elongated parallelepiped with an open top in the central part of which electrode blanks are horizontally stacked and covered with an insulating bulk material. The gaps between the granules of the insulating material are filled with flue gases.

The furnace is connected to a constant electric current source by the graphite current leads that are located at the ends of the furnace. The heating of electrode blanks occurs due to Joule heat and exothermic chemical reactions. The heat released in the furnace is also consumed for heating the enclosing elements, with endothermic chemical reactions and losses to the environment. An intensive evaporation of moisture happens during the heating of the furnace and leads to an abrupt change in the physical properties of the bulk insulating material.

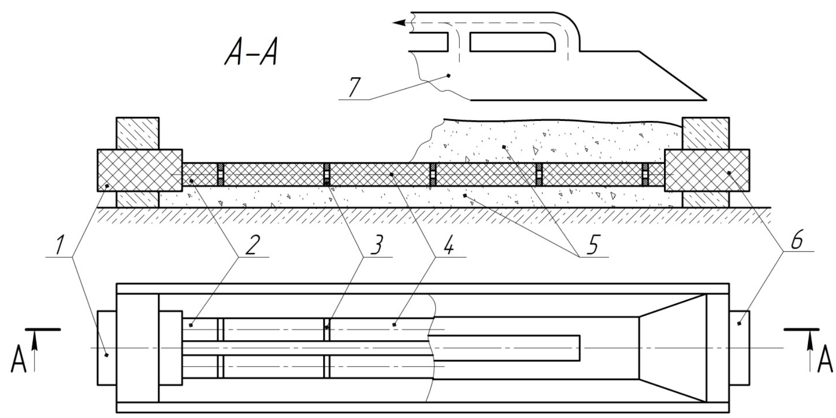

Fig. 1. A diagram of the Castner furnace for graphitization: 1 and 6 are the front and rear current leads, respectively; 2 denotes compensatory inserts; 3 shows ring-shaped electrical contact pads; 4 denotes electrode blanks; 5 is the thermal insulation charge; 7 is a shelter for the removal of gases

Evaporation of moisture in the furnace heating process begins in the furnace central portion at the periphery of the blanks at their contact with the granular insulation. The steam expands and moves the non-evaporable unrelated moisture to peripheral cold layers of insulation, where it condenses. Further evaporation of moisture is accompanied by its ejection to the walls and the floor of the furnace, the condensation of steam in less heated layers of the heat insulating charge, and its partial evacuation into the environment. The condensed water in the heat insulating charge moves down under gravitation forces, thereby increasing the concentration of moisture in the thermal insulation of the hearth bottom. The steam, which has been produced by the evaporation of moisture in the bottom and side parts of the insulation, almost fully passes through the heated central portion of the furnace. Consequently, at high temperatures (over 650 °C), there is a conversion of the water vapour, accompanied by gasification of the carbonaceous material mainly in the contact area of the electrode blanks with the insulating charge, and much of the heat is absorbed due to the following main reactions [9, 10] (at ~800 °C):

$$C+H_2O \rightarrow CO+H_2 \ (-118 \text{ kJ/mol}), \quad (1)$$

$$C+H_2O \rightarrow CO+H_2 \ (-118 \text{ kJ/mol}), \quad (2)$$

$$C+CO_2 \rightarrow 2CO \ (-161 \text{ kJ/mol}). \quad (3)$$

The gasification reaction products – carbon monoxide and hydrogen – are partially evacuated to the environment and partially, while passing through less heated layers of the insulation, react exothermically to form water and methane through the following main reactions [13, 14] (at an insulation temperature of ~200 °C):

$$CO+3H_2 \rightarrow CH_4+H_2O \ (+206 \text{ kJ/mol}), \quad (4)$$

$$2CO+2H_2 \rightarrow CH_4+CO_2 \ (+247 \text{ kJ/mol}), \quad (5)$$

$$CO_2+4H_2 \rightarrow CH_4+2H_2O \ (+165 \text{ kJ/mol}), \quad (6)$$

$$2CO \rightarrow C+CO_2 \ (+172 \text{ kJ/mol}). \quad (7)$$

The conversion of the carbon monoxide and the hydrogen produces water that further condenses and, under the influence of gravitational forces, moves down to the bottom insulation, where it evaporates again. Thus, due to the mechanism of the moisture and vapour movement and the mechanism of the carbonaceous material gasification, the water and the steam circulate through the furnace volume to complete their evacuation into the environment.

The above-listed chemical reaction equations (1)–(7) show that most of them can be both direct and reverse. The direction of these reactions depends on the temperature and the equilibrium constants [13, 14].

At temperatures above 3,200 K, the carbonaceous materials of the furnace are sublimated. The elements of the furnace design produce a thermoelectric power contact interaction.

5. A mathematical model of the graphitization process

The developed mathematical model of the thermoelectric power state of the Castner furnace is based on a physical model of the graphitization process.

A distinctive feature of the developed mathematical model and the model presented in [15] is an opportunity to take into account the mechanisms of the moisture and vapour transportation, the heat transfer due to the gasification reactions of the carbonaceous material in the furnace, and the conversion of the carbon monoxide and the hydrogen in the insulating charge.

The system of nonlinear differential equations describing the thermoelectric power field of the Castner furnace can be represented by the following generalized statement:

$$\begin{cases} \dfrac{\partial H}{\partial \tau} = \nabla \cdot \left[\lambda_{eff}(p,T) \nabla T(X) \right] + \chi(p,T) \left| \nabla U(X) \right|^2 + q_{V,chem} + q_{V,devapor}; \\ \nabla \cdot \left[\chi(p,T) \nabla U(X) \right] = 0, \end{cases} \quad (8)$$

where

$$H = \int_{T_{ref}}^{T} c_p^{eff}(T) \rho(T) dT$$

is a full volume enthalpy that takes into account the heat of evaporation or condensation in water-containing materials, or the heat of sublimation of carbon-containing materials of the furnace, J/m^3; τ is the time, s;

$$c_p^{eff}(T) = \begin{cases} c_{p-0}^{*}(T), \quad T < T_{eqL}; \\ \dfrac{c_{p-0}^{*}(T_{eqL}) + c_{p+0}(T_{eqR})}{2} + \dfrac{L_{fm}}{\Delta T}, \quad T_{eqL} \le T \le T_{eqR}; \\ c_{p+0}(T), \quad T > T_{eqR}, \end{cases}$$

where $c_p^{eff}(T)$ is the effective mass isobaric heat capacity that takes into account the heat capacity of the water and the heat of its evaporation in the presence of moisture in the materials; in graphitized materials, it is the heat of graphite sublimation at high temperatures, J/(kg×K); T_{eqL}= =T_{eq}–ΔT/2; T_{eqR}=T_{eq}+ΔT/2; T_{eq} is the equilibrium temperature of the evaporation, sublimation (the first order phase transition) or chemical reaction, K; ΔT is the temperature interval of smoothing [16], K; c_{p-0}^{*} is the mass heat capacity of the material depending on its water content, J/(kg×K);

$$L_{fm} = \begin{cases} \alpha_w L_{fw} - \text{at the moisture evaporation}; \\ (1-\alpha_w) L_{fw} - \text{at the graphite sublimation}; \end{cases}$$

where L_{fm} is the mass heat in the first order phase transition, J/kg; α_w is the mass fraction of water in the wet material; L_{fw} and L_{fs} are the latent heat at the water evaporation and the latent heat at the graphite sublimation, respectively, J/kg; ρ is the density of the material, kg/m^3; ∇ is the Hamiltonian operator, m^{-1}; $q_{w,chem}$ is the density of the internal heat source associated with the chemical reactions (1)–(12) [13], W/m^3; $X(x,y,z) \in R^3$ is the Cartesian coordinate system, m; $q_{w,devapor}$ is the density of the internal heat source that takes into account the heat and mass transfer of the water vapour and its condensation, W/m^3.

Enthalpy takes into account the moisture content of the thermal insulation and the heat of sublimating the carbonaceous materials of the Castner furnace on the basis of the above-given relation of $c_p^{eff}(T)$; it is defined as follows:

$$H = \int_{0}^{T_{eqL}} c_{p-0}^{*}(T) \rho_{-0}^{*}(T) dT + \\ + \frac{\left[c_{p-0}^{*}(T_{eqL}) \rho_{-0}^{*}(T_{eqL}) + c_{p+0}(T_{eqR}) \rho_{+0}(T_{eqR}) \right]}{2} \Delta T + \\ + L_{fv} + \int_{T_{eqR}}^{T>T_{eqR}} c_{p+0}(T) \rho_{+0}(T) dT, \quad (9)$$

where c^*_{p-0}, ρ^*_{-0} and c_{p+0}, ρ_{+0} are the properties of the materials on both sides, depending on the phase transition temperature (taking into account the moisture content), respectively;

$$L_{fv}=\begin{cases}\alpha_w\rho_w L_{fw} - \text{ at the moisture evaporation;}\\ (1-\alpha_w)\rho_g L_{fs} - \text{ at the graphite sublimation,}\end{cases}$$

where L_{fv} is the volumetric heat of the first order phase transition, J/m^3; ρ_w and ρ_g are the densities of water and graphite, respectively, in kg/m^3.

The effective thermal conductivity of the material, taking into account the moisture content, is determined by the dependence:

$$\lambda_{eff}(p,T)=\begin{cases}\lambda_{-0}(p,T), \ \ T<T_{eqL};\\ \lambda_{-0}(p,T_{eqL})+\dfrac{\lambda_{+0}(p,T_{eqR})-\lambda_{-0}(p,T_{eqL})}{\Delta T}T,\\ \lambda_{+0}(p,T), \ \ T>T_{eqR},\end{cases}$$

$$T_{eqL}\le T\le T_{eqR}, \quad (10)$$

where λ_{-0} and λ_{+0} mean thermal conductivity of the material on both sides, depending on the phase transition temperature, respectively, W/(m×K); p is the pressure, Pa.

The density of the internal heat source, which is associated with chemical reactions during the gasification of the carbonaceous material, is described by the equation:

$$q_{Vchem}=\frac{Q_{r.g}m_{g.vapor}}{V_{gasific}\tau_{gasific}}, \quad (11)$$

where $Q_{r.g}$ is the thermal effect of the gasification reaction, J/kg; $m_{g.vapor}$ is the mass of the vapour in the gasification reaction, kg; $V_{gasific}$ is the volume of the gasification zone, m^3; $\tau_{gasific}$ is the duration of the gasification process, s.

Assuming that the principal reaction in the gasification process is the reaction of "water gas" (1), the $Q_{r.g}$ value is determined by (12) [13], and $m_{g.vapor}$ is estimated by (13).

$$Q_{r.g}=(-7{,}165{,}100-718.25T+ +0.1162T^2+0.00007903T^3), \quad (12)$$

$$m_{g.vapor}=1.5m_C=1.5\min\begin{pmatrix}ke^{-\frac{E}{RT}}m_{Cgasif}\tau_{gasific}\\ 0.6667m_{all.vapor}\end{pmatrix}, \quad (13)$$

where T is the absolute bulk temperature of carbon in the gasification zone, K; m_C is the mass of carbon in the gasification reaction [14], kg; k is the pre-exponential factor, s^{-1}; E is the activation energy, J/mol; R is the gas constant, J/(mol×K); $m_{Cgasific}$ is the mass of carbon in the gasification zone, kg; $m_{all.vapor}$ is the mass of water vapour passing through the gasification zone, kg.

The density of the internal heat source, taking into account the mass transfer of the water vapour and its condensation, can be determined by the equation:

$$q_{V,devapor}=\frac{m_{vapor}L_{fv}\xi_{evac.p}}{V_{cond}\tau_{cond}}, \quad (14)$$

where m_{vapor} is the mass of the evaporated water, kg; $\xi_{evac.g}$ is the coefficient that takes into account the evacuation of vapour into the environment; V_{cond} is the volume of the steam condensation zone, m^3; τ_{cond} is the duration of the condensation process, s.

The initial conditions at τ=0 are:

$$\begin{cases}T=0;\\ U=0,\end{cases} \quad (15)$$

where U is the voltage, V.

The boundary conditions at τ>0 are:

– at the ends of the furnace current leads:

$$j_n(\tau)\big|_{shunt}=\mathbf{n}\cdot(-\chi(p,T)\nabla U)\vee U\big|_{shunt}=U(\tau), \quad (16)$$

where j is the current density, A/m^2; **n** is the vector of the external normal to the surface of the electrical power supply; χ is the material conductivity, S;

– on the outer surfaces of the furnace bordering on the environment:

$$\begin{cases}\mathbf{n}\cdot(-\lambda(p,T)\nabla T)=\alpha_{eff}(T)(T-T_{env});\\ \mathbf{n}\cdot\nabla U=0,\end{cases} \quad (17)$$

where α_{eff} is the effective heat transfer coefficient, W/(m^2·K); T_{env} is the absolute ambient temperature, K;

– the conditions of the thermoelectric power contact between the elements of the furnace design are as follows:

$$\begin{cases}\{T\}=\mathbf{n}\cdot(r_\lambda\mathbf{q});\\ \{\mathbf{n}\cdot\mathbf{q}\}=0;\\ \{U\}=\mathbf{n}\cdot(r_e\mathbf{j});\\ \{\mathbf{n}\cdot\mathbf{j}\}=0,\end{cases} \quad (18)$$

where r_e is the specific electrical resistivity, Ohm·m; r_λ is the specific thermal resistance, (m^2·K)/W; **q** is the vector of the heat flux density, W/m^2; **j** is the vector of the electric current density, A/m^2.

6. A method of the numerical solution of the thermoelectric power problem

The main source of the Castner furnace heating is the Joule heating released while the electric current is passing through the carbon blanks. The second important source of heating is a heat of the chemical reactions of converting the water vapour, the carbon monoxide and the hydrogen in the insulation. According to (8), the quantity of the released Joule heating depends on the square of the electric field strength ($E=-\nabla U$, W/m) and the electrical conductivity of the materials, which in turn depend on the temperature and the pressure. The experimental data on the two-parameter dependence of electrical conductivity χ(T, p) of the carbonaceous materials [13] show that within the temperature and pressure changes in the bulk carbon materials of the Castner furnace the dependence of the electrical conductivity on temperature changes is much greater than on pressure changes. In determining the electrical conductivity, the pressure in the bulk layer is taken as hydrostatic.

The numerical solution of the nonlinear problem (8)–(18) is based on the finite element method [17]. The problem is solved iteratively, using the Newton method of linearization [18, 19].

Discretization of the computational domain is performed with linear tetrahedral elements, using free open source software for automated generation of the Gmsh mesh [20]. The thermoelectric power problem is solved while using software of our own development [19, 21], previously tested for accurate numerical solutions. The computational grid parameters (the number of finite elements, or nodes) are determined on the basis of the double conversion [18]. The numerical experiments have resulted in the following sampling of the computational domain (1/4 of the furnace): 150,153 tetrahedral finite elements and 72,599 nodes.

7. Verification of the mathematical model of the direct heating furnace

The comparative analysis of the results of the numerical simulation and the physical experiments to determine the temperature fields in the Castner furnace [22] is carried out by comparing the mean temperature values that have been determined by three points on the periphery of the electrode blanks in a variety of cross-sections (Fig. 2–4). According to the physical experiment, the relative deviation in temperature values data in each of the examined sections of the blanks is about 3 % of their average value, and for the numerical experiment, it does not exceed 1 %.

The upper limit of the compared temperatures (1,600 °C) in the graphs in Fig. 2–4 is connected with the measuring characteristics of temperature sensors that are used in the physical experiment in the Castner furnace [22].

The dependence of the change in the average temperatures of the specific energy consumption (SEC) in the cross section of the central workpiece of the right candle for the middle part of it is shown in Fig. 2, whereas the end portion thereof is specified in Fig. 3.

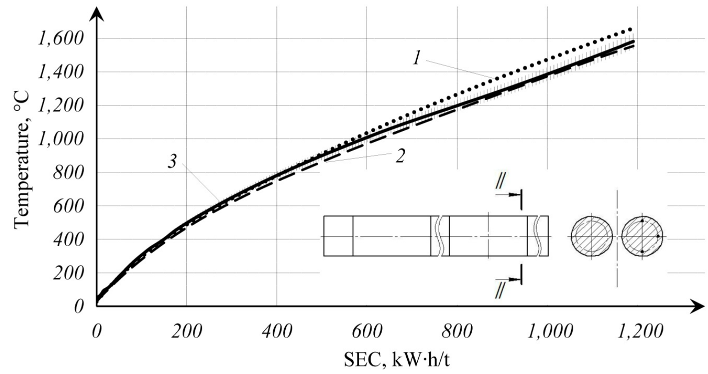

Fig. 3. A change in the average temperature in the cross section of the butt end of the central workpiece of the right candle, depending on the SEC: 1 is the numerical simulation excluding the thermal effects of the material's chemical gasification reactions; 2 is the numerical simulation based on the thermal effects of the material's chemical gasification reactions; 3 is the experiment (δ_t=3 %)

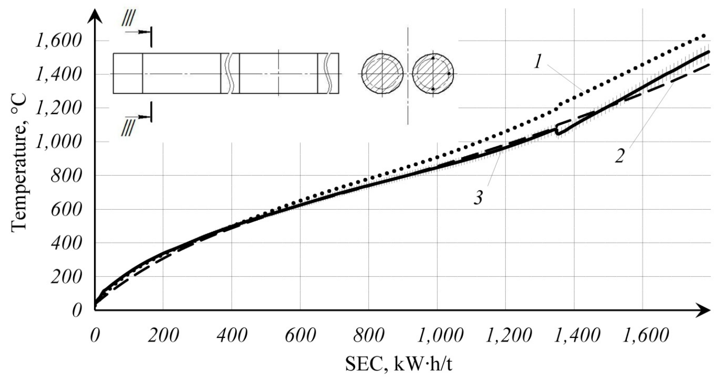

Fig. 4. A change in the average temperature in the cross section of the butt end of the outermost workpiece of the right candle, depending on the SEC: 1 is the numerical simulation excluding the thermal effects of the material's chemical gasification reactions; 2 is the numerical simulation based on the thermal effects of the material's chemical gasification reactions; 3 is the experiment (δ_t=3 %)

The dependence of the average values of the temperature increase on the SEC in the cross-section of the butt end of the outermost blank of the left candle is shown in Fig. 4.

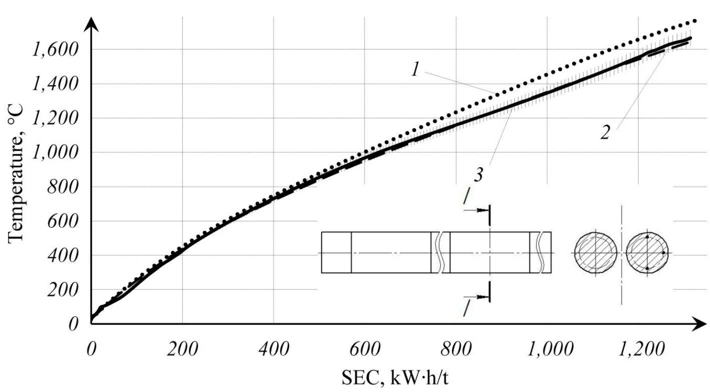

Fig. 2. A change in the average temperature in the cross section of the middle part of the central workpiece of the right candle, depending on the SEC: 1 is the numerical simulation excluding the thermal effects of the material's chemical gasification reactions; 2 is the numerical simulation based on the thermal effects of the material's chemical gasification reactions; 3 is the experiment (δ_t=3 %)

As a result of comparing the data of the numerical analysis with the experimental data (Fig. 2–4), it has been found that the difference between the calculated and experimental data does not exceed 4 % in the temperature range of up to 1,600 °C for option calculations that take into account the impact of thermal effects of the chemical gasification reactions. Otherwise, when there is no influence of the thermal effects of the chemical reactions of gasification in the numerical model of the furnace, the deviation from the experimental data is more than 10 %.

8. The discussion of the results of the numerical modelling of the physical fields in the Castner furnace

The advantages of the completed numerical analysis of the physical state of Castner furnaces during graphitization of electrodes include taking into account the effect on the temperature fields' formation produced by the following factors: the thermal effects of the gasification reactions of the carbonaceous material, the conversion of the carbon monoxide and the hydrogen in the heat-insulating material, and the heat and mass transfer of moisture. The main limitation of this study may be the use of empirical relationships to account for the above-listed factors.

The undertaken tests are necessary for the development of energy-saving regulations of the electrical power input in the existing Castner furnaces, either for upgrading their designs to check serviceability or for switching to the graphitization of new electrode products.

The study of the physical fields in the process of graphitizing electrode blanks in Castner furnaces is a continuation of the authors' previously published scientific works. These works are devoted to the method of a numerical solution of the simulation problems [19], a numerical analysis of the physical fields of electrolysers [21], Acheson furnaces [4] and Castner furnaces [15], as well as experimental research on their thermal state [22].

9. Conclusions

1. The analysis of the physical and chemical processes that occur during the graphitization of electrode products in Castner furnaces has helped formulate the thermoelectric power physical model of the furnace to take into account the thermal effects of the chemical reactions, vaporization, condensation, graphite sublimation, and a thermoelectric power contact interaction between the furnace design elements.

2. A mathematical model is formulated to simulate the thermoelectric power state of the Castner furnace in the process of graphitizing electrode blanks while taking into account the thermal effects of the carbonaceous material gasification reactions, the conversion of the carbon monoxide and the hydrogen in the thermal insulation material, the heat and mass transfer of moisture, sublimation of graphite, and contact interaction between the furnace design elements of thermoelectric nature. The suggested mathematical model is used to develop a corresponding numerical model of the thermoelectric state of the Castner furnace by the authors' software, built on the finite element method.

3. The verification of the numerical model of the thermoelectric state of the Castner furnace has showed a 4 % deviation in the concordance between the results of the numerical modelling of temperature fields and the findings of a physical experiment at the temperature change range of up to 1,600 °C for the case of taking into account the impact of thermal effects of chemical gasification reactions. Otherwise, excluding the thermal effects of gasification, the difference between the numerical and experimental data constitutes more than 10 %.

References

1. Sang-Min, L. Bulk graphite: materials and manufacturing process [Text] / L. Sang-Min, K. Dong-Su, R. Jea-Seung // Carbon Letters. – 2015. – Vol. 16, Issue 3. – P. 135–146. doi: 10.5714/cl.2015.16.3.135
2. Fialkov, A. Processes and equipment for production of powdered carbon materials [Text] / A. Fialkov. – Moscow: Aspect Press, 2008. – 687 p.
3. Kuznetsov, D. The graphitization process of carbon materials. Modern research methods [Text] / D. Kuznetsov, V. Fokin. – Novocherkassk: PSRSPU, 2001. – 132 p.
4. Kutuzov, S. V. Making the Heat-Insulating Charge of Acheson Graphitization Furnaces More Efficient [Text] / S. V. Kutuzov, V. V. Buryak, V. V. Derkach, E. N. Panov, A. Ya. Karvatskii, G. N. Vasil'chenko et. al. // Refractories and Industrial Ceramics. – 2014. – Vol. 55, Issue 1. – P. 15–16. doi: 10.1007/s11148-014-9648-5
5. Znamerovskij, V. Mathematical modelling of the graphitization process [Text] / V. Znamerovskij. – Moscow: Metallurgija, 1994. – 64 p.
6. Yarymbash, D. Identification of the electrical parameters of the circuit loop of powerful graphitization furnaces [Text] / D. Yarymbash // Electronics & electrical engineering. – 2012. – Vol. 1. – P. 49–54.
7. Yarymbash, D. S. On specific features of modeling electromagnetic field in the connection area of side busbar packages to graphitization furnace current leads [Text] / D. S. Yarymbash, A. M. Oleinikov // Russian Electrical Engineering. – 2015. – Vol. 86, Issue 2. – P. 86–92. doi: 10.3103/s1068371215020121
8. Yarymbash, D. Energy analysis of the structure of the end joints of lateral tire packages and current leads of graphitization furnaces [Text] / D. Yarymbash, A. Oleinikov // Electronics & electrical engineering. – 2013. – Vol. 2. – P. 26–34.
9. Pieklo, J. Analysis of the state of stress in the connection of graphite electrodes [Text] / J. Pieklo, M. Maj // Archives of foundry engineering. – 2015. – Vol. 15, Issue 1. – P. 85–88.
10. Yonggang, L. Numerical simulation analysis on lengthwise graphitization furnace co-production silicon carbide [Text] / L. Yonggang, H. Yangdong, W. Lianying, Y. Chunli // Advanced Materials Research. – 2012. – Vols. 557-559. – P. 835–838. doi: 10.4028/www.scientific.net/amr.557-559.835
11. Chong, Sh. Numerical study on the heat recovery and cooling effect by built-in pipes in a graphitization furnace [Text] / Sh. Chong, Zh. Maoyong, L. Xianting // Applied Thermal Engineering. – 2015. – Vol. 90. – P. 1021–1031. doi: 10.1016/j.applthermaleng.2015.04.036
12. Belenchenko, V. Simulation of physical and chemical processes of high-temperature processing of carbon products in Acheson's furnaces [Text] / V. Belenchenko // Solid Fuel Chemistry. – 2009. – Vol. 1. – P. 51–57.

13. Higman, C. Gasification [Text] / C. Higman, M. van der Burgt. – London: Elsevier Science & Technology Books, 2008. – 456 p.
14. Basu, P. Biomass gasification and pyrolysis: practical design and theory [Text] / P. Basu. – London, New York : Published by Elsevier Inc., 2010. – 365 p. doi: 10.1016/b978-0-12-374988-8.00001-5
15. Karvatskii, A. Estimated study the implementation of the direct graphitization process on PJSC "Ukrgrafit". Herald of NTUU "KPI" [Text] / A. Karvatskii, I. Shilovich, S. Kutuzov et. al. // Chemical engineering, ecology and resource saving. – 2008. – Vol. 1, Issue 1. – P. 42–46.
16. Arutjunjan, R. Integral Equations of the Stefan Problem and Their Application in Modeling of Thawing Soil [Text] / R. Arutjunjan // Science and Education of the Bauman MSTU. – 2014. – Vol. 15, Issue 10. – P. 419–437. doi: 10.7463/1015.0814769
17. Zenkevych, O. Finite element method in engineering [Text] / O. Zenkevych. – Moscow: Myr, 1975. – 543 p.
18. Kalitkin, N. Numerical methods: tutorial [Text] / N. Kalitkin. – BHV-Petersburg, 2011. – 586 p.
19. Karvatskii, A. Solution of the problem of nonlinear non-stationary heat conductivity by finite element method [Text] / A. Karvatskii, A. Pedchenko // Journal of Azov State Technical University. Series: Technical science. – 2014. – Vol. 32. – P. 205–214.
20. A three-dimensional finite element mesh generator with built-in pre- and post-processing facilities [Electronic resource]. – Available at: http://geuz.org/gmsh/
21. Urazlina, O. Yu. Efficiency analysis of the use of highly graphitized bottom blocks in 156 – 160 kA aluminum electrolyzers [Text] / O. Yu. Urazlina, V. I. Churilin, E. N. Panov, G. N. Vasil'chenko, A. Ya. Karvatskii // Refractories and Industrial Ceramics. – 2005. – Vol. 46, Issue 2. – P. 93–97. doi: 10.1007/s11148-005-0059-5
22. Leleka, S. The study of uneven temperature field in billet electrodes during their graphitization in the Castner furnace [Text] / S. Leleka, T. Lazariev, A. Pedchenko, D. Shvachko // Eastern-European Journal of Enterprise Technologies. – 2015. – Vol. 6, Issue 5 (78). – P. 28–32. doi: 10.15587/1729-4061.2015.56642